/lmg - 0039a

PS/BT/Note 84-3
8.2.1984

DESIGN PROPOSAL FOR A LEAR BUMP

D. Grier, K.D. Metzmacher

1. SUMMARY

This proposal describes the design and expected performance of a fast bump for the injection of H^-/H^0 into LEAR. The magnets will be situated in SS 41 and SS 42 of the LEAR ring.

The design is based on the use of two multiturn lumped inductance magnets. The magnets are exterior to metallised ceramic vacuum chambers.

The two magnets will be pulsed from twin lumped element pulse forming networks of Z_o = 15 Ohms, which charged from a common power supply to 28 kV, will be discharged via appropriately timed main, dump and clipper thyratron switches.

2. INTRODUCTION

The injection of H^-/H^0 into LEAR has been studied by P. Lefevre and D. Möhl[1)]. The scheme requires a local closed orbit deformation in SL4 which will bump the circulating beam close to the stripping target on which the incoming beam is stripped. The fast bump kickers will be symmetrically disposed up and downstream of the target and will have a bending power of 100 Gm.

The study of (1) suggests reusing the magnets and pulse generator from the reclaimed PS 50 MeV monoturn injection equipment KM 30. We have studied this proposal and have come to the conclusion that whereas the magnets are reusable, the power supply is not; this for reasons of lack of kick strength, pulse length, flexibility and components (only one pulser is available). New pulse generators, based as far as possible on existing designs and new controls compatible with the LEAR control system should be built.

The present proposal is based on the information given in Table 1.

3. DESIGN PROPOSAL

A simplified schematic of one magnet with its pulse generator is shown in Figure 1. The artificial PFN (lumped L's and C's) of two such circuits will

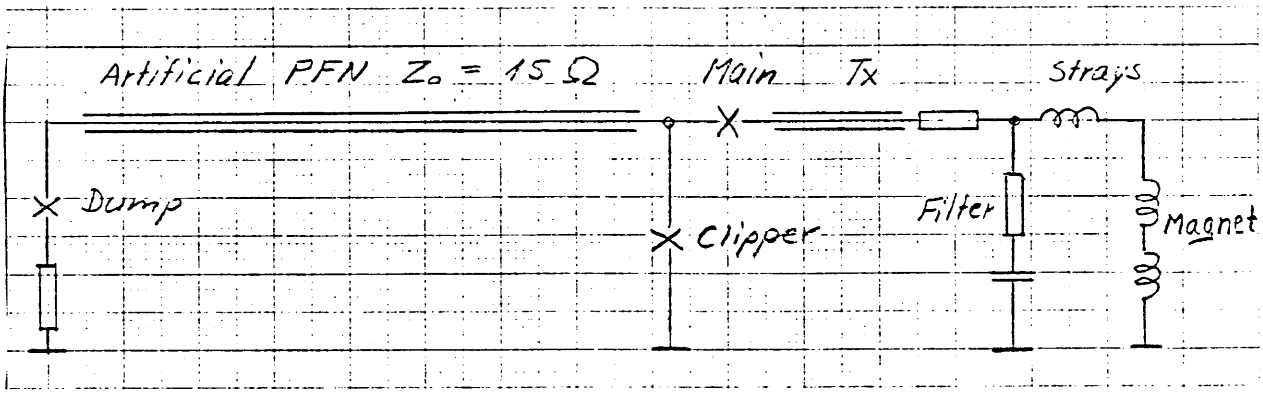

Figure. 1. Schematic of one fast pulse circuit

be charged by a common resonant charging power supply, as shown simplified in Figure 2.

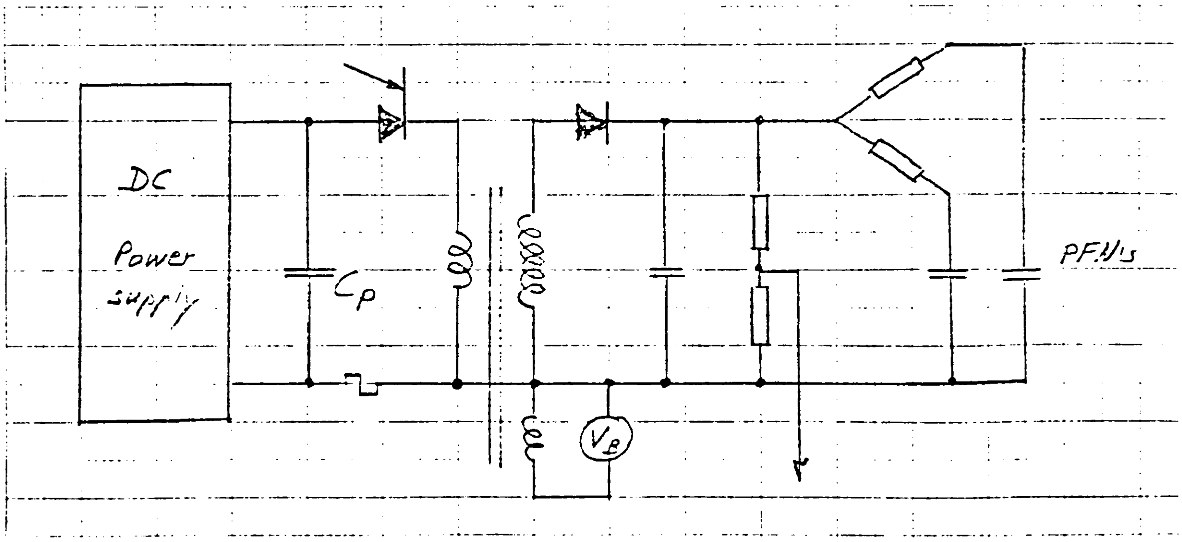

Figure 2. Schematic of charging circuit for PFN's

The duration of the bump will be variable over the range of zero to 24 μsecs without degradation of rise or fall times. Since each magnet is pulsed from an independant PFN, synchronisation will be necessary and has to take particle flight time into account.

Thyratron switching using double ended CX 1154 B tubes for dump and clipper application is proposed. These tubes are more complicated than single ended tubes but are necessary to prevent damage resulting from possible equipment malfunctioning (reverse currents). The main switch however will not be required to pass reverse current and thus a simpler CX 1159 tube is proposed.

The two pulse forming lines will be housed together with all thyratrons and dump terminators in one large oil tank. The volume of transformer oil (Shell Diala C) will be ≈ 2 m^3 and has to be water cooled via a heat exchanger. The high voltage resonant pulse transformer will be external but close coupled.

The floor area around the tank assembly should be oil tight and a small oil retaining wall will be needed.

3.1 Magnet

The magnets were originally designed for duty as KM 30 [2]. Because of the moulded construction it is not possible to improve their performance. A cross-section drawing is given in Figure 3. From this the wiring arrangement can be seen. It is also evident that the magnet is built-up from C-cores, making it easily mountable and dismountable around the vacuum chamber. The magnetic circuit is split on the vertical centre line so that the longitudinal coupling impedance is minimised. The split is alumimium filled, thus presenting an efficient eddy current shield.

The horizontal field-distribution on the median plane has been calculated for nominal excitation and measured at very low excitation, both curves are presented in Figure 4, from which the useful horizontal aperture can be measured.

The magnet is designed to be installed outside machine vacuum (in fact it will be the only fast PS kicker magnet which is not in vacuum). This requires the use of a ceramic vacuum chamber because a metal chamber will seriously attenuate and disperse the fast magnetic fields. However, the chamber must be electrically conductive and the ceramic has to be metallised. At present the actual amount and quality (for bakeable UHV) of this metallisation are under discussion and tests are prepared to measure the effect. Therefore the present note cannot take into account quantitively this effect. Qualitatively, the magnetic field rise and fall times will suffer.

In order to re-employ as many components as possible and to arrive at a coherent design we propose to connect the two half-magnet windings in series. This makes the total magnet inductance rather high, but halves the magnet current requirement. Because of the backleg winding construction the stray inductance is relatively high, amounting to ≈53% of the "useful" inductance.

The magnet will be terminated at its high voltage end. The terminator will be oil filled and forced cooled. The RC filter (Figure 1), the capacitance of which will be finally chosen to give the best magnetic field performance inside the metallised ceramic vacuum chamber, will be integrated into the terminator.

The terminator to magnet connection will be via short high voltage cables with easily demountable plug and socket arrangements.

The magnet design parameters and the performance predicted are given in Table 2.

3.2 Pulse forming network

The design of the PFN is closely based on the Continuous Transfer pedestal pulse generator design. In particular the (spare) capacitors will be used and the resonant charging circuit will be copied.

It is intended to place both the PFN's required in one large tank together with the six thyratrons. The PFN impedance will be 15 Ohms, and with 10 cells a maximum output pulse flat top of 24 μsecs will be possible. The nominal magnet current will be 900 A for a charging voltage of 28 kV.

The PFN design parameters are given in Table 3 and a detailed electrical circuit for the design studied, is given in Figure 5. A front cell is included to provide more switching-on current and thus achieve a faster field rise with some overswing and more useful pulse length.

3.3 Thyratron switches

To achieve the required output pulse shape three thyratron switches are needed : the first, called main switch, discharges the PFN into the short transmission cables towards the load. The second, placed at the far end of the PFN, is called the dump switch and is needed for pulse length control and usually produces the pulse fall, at the same time dumping the unwanted pulse length into the dump terminator. However, in the present case, because a lumped element PFN is used, the initial dump switch fall time will be degraded. It is therefore essential to use a clipper switch. This switch is placed at the front of the PFN and when triggered short circuits (clips) the PFN, thus provoking a rapid voltage fall; when this happens the clipper must conduct twice the nominal magnet current. (Obviously, to be effective, the clipper must switch before the dump generated fall arrives at the PFN front.)

To limit the I.t product passed by the clipper the timing between the dump and clipper switches should be tuned and ganged.

In case of equipment malfunctioning, missing or incorrect timing of the various switches it is very likely that large reverse currents will have to be passed by the dump and/or clipper switch. Particular attention is placed on the correct choice of thyratron. We propose to use an ordinary EEV CX 1159 glass tube in the main switch application, there being many partially used tubes in stock. For both dump and clipper positions EEV CX 1154 B ceramic single stage double ended tubes will have to be bought.

3.4 Power supply

Since the total PFN capacity to be charged is identical to that of the Continuous Transfer Pedestal generators it is proposed that a pedestal type resonant charging power supply be used. The HV transformer in the pedestal generator is housed in the PFN tank. In order to accomodate the additional thyratrons and dump terminators for the LEAR bump generator it will be necessary to purchase a transformer with its own tank, which will be closely coupled to the PFN tank via a bellows and flange.

3.5 Controls

The two pulse generators should be coupled such that the control protocol is identical to that for one of the existing LEAR injection kickers. There will be no separate oil controls, the oil pump being linked to the power ON command. The controls interface unit should be identical to that of the injection kicker, so that the control software can be "cloned".

Four timing pulses - two "main" and two "clipper" will be required to determine the delay and length of each bump; one 'SCR' pulse preceeding those pulses by about 10 msecs. will be necessary for PFN charging.

Remote monitoring should be made via the existing kicker monitoring system.

4. PERFORMANCE

A typical magnet current pulse is shown in Figure 6 for several different fall time conditions. The rise time is always produced by the main switch and is the same for all conditions.

The fastest fall time is that produced by the clipper switch and is practically independant of pulse length.

The medium fall time is that produced by the dump switch when the clipper is not triggered. This fall time is also independant of pulse length.

The third, slowest, fall time is the so-called free fall, i.e. that produced by the reflection of the backward travelled main switch wave. It is produced with only the main switch operating and represents the longest pulse width obtainable.

Details of the rise time and fall time using the clipper switch are given in Figures 7 and 8, respectively. Considering Figure 1, we can see that basically the magnet current rise and fall times (and thus the magnetic field) are exponential and further somewhat surprising, that the fall time-constant $\tau_f = L/R_{Load}$ is intrinsically twice that of the rise time $\tau_r = L/(R_{PFN} + R_{Load})$.

5. COST ESTIMATES (non exhaustive)

	kFS
HV charging power supply	36
Controls	25
Switches	40
PFN + cooling	55
Installation	5
Terminators	5
Regie labour	40
	206 kFS

6. REFERENCES

1. D. Moehl and P. Lefèvre, private communication
2. "Analysis of the 50 MeV injection region in connection with the proposed modifications of vacuum chambers in the PS", M. Weiss, MPS/LIN/Note 72-7.

Distribution :

BT Group staff
Lear Group staff
PS Group Leaders
D. Dekkers (Divisional Safety Officer)

TABLE 2 - Design parameter and performance list

Magnet	Number of magnets/section		1	
	Type		Lumped inductance	
	Construction		double C-core with one 4-turn backleg winding each. Windings connected in series	
	Magnet box size without connections	w h l	351 197 225	mm mm mm
	Physical aperture	w h l	180 85 225	mm mm mm
	Ferrite type		Philips 4A4	
	Inductance	total strays effective	13.77 4.77 9	µH µH µH
	Ferrite length Effective magnetic length		150 190	mm mm
	Useful horizontal Field region	±1% ±0,5%	±40 ±24	mm mm
	Nominal kicker strength Nominal excitation Nominal $\int Bd\ell/kV_{PFN}$		100 900 x 4 3.6	Gm A.turns Gm/kV
	Corresponding air gap flux density Mean ferrite flux density Mean $\int Bd\ell$		524.5 2137 > 0,5	G G Gm
	$\int Bd\ell$ rise time	(5 - 95)% (10 - 90)%	1.0 0.84	µs µs
	$\int Bd\ell$ fall time	(95 - 5)% (90 - 10)%	2.4 1.85	µs µs
	$\int Bd\ell$ flat top ripple		+ 5.75 - 2.73	% %
	Terminator		15	Ohm
	Compensation	RC	15 8.2	Ohm nF

Attention : Performance related to $\int Bd\ell$ pulse shape are given for magnet without metallised ceramic vacuum chambers.

TABLE 3. PFN parameter list

Pulse Forming Network	Type		Lumped elements	
	Construction		10 cells + front cell	
	Each cell	L C	19,6 87	μH nF
	Front cell	C R L	43,5 15 19,6	nF Ohm μH
	Impedance		15	Ohm
	Main switch Dump + Clipper switches		EEV CX 1159 EEV CX 1154B	
	Pulse length	Max.	24	μs
	PFN voltage	Nominal Max.	27.8 33	kV kV
	Rep rate	Nominal Max.	4 1.2	secs secs
	Tank size	w l h	1.2 2.1 0,9	m m m
	Isolating + cooling oil Shell Diala C		≈ 2	m^3
	HV transfo separate		≈ 1	m^3
Terminators	Construction		Allen Bradley carbon mass discs	
	Power dissipation @ 0,25 Hz		73	W

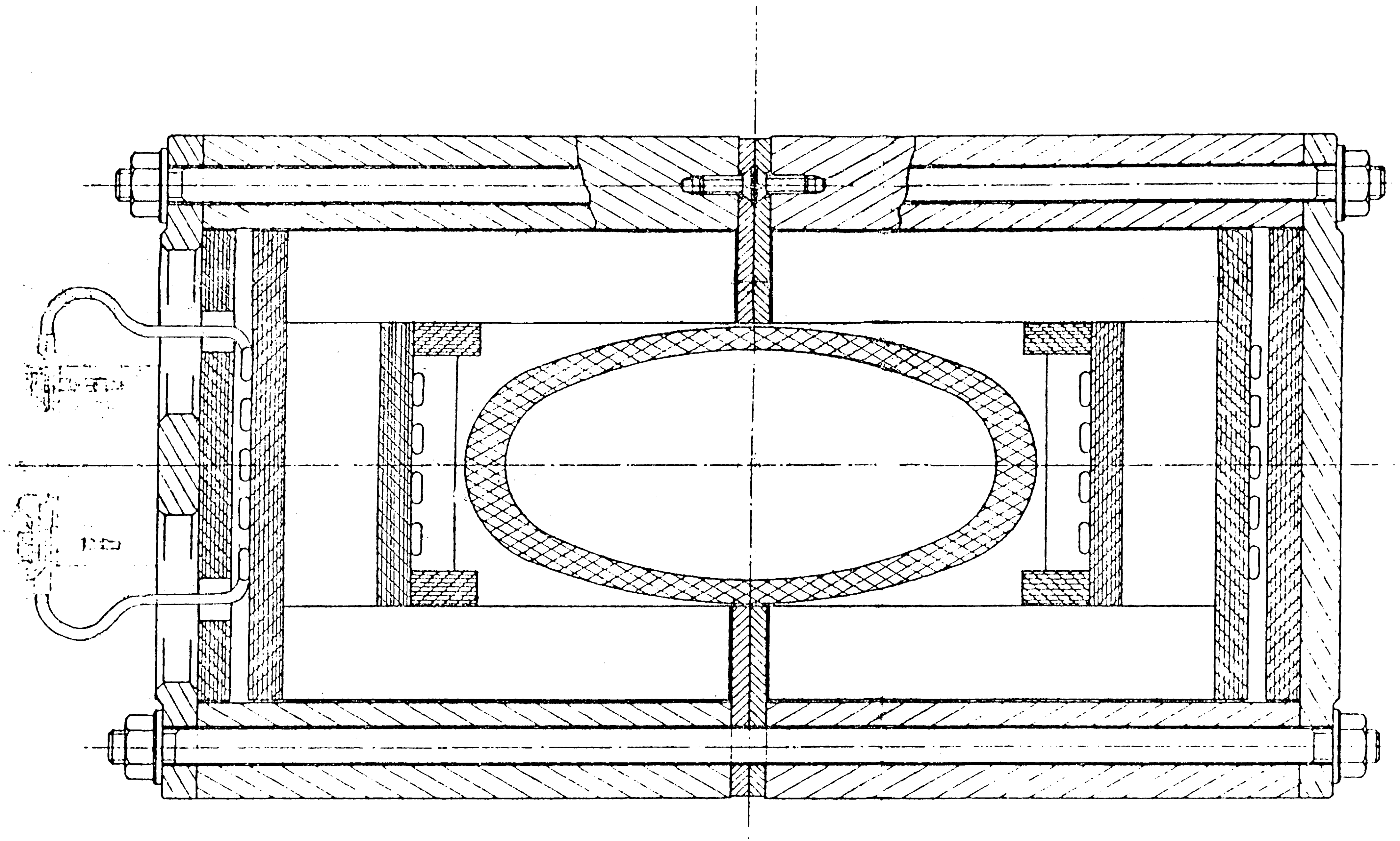

Fig.3. Cross section of magnet construction

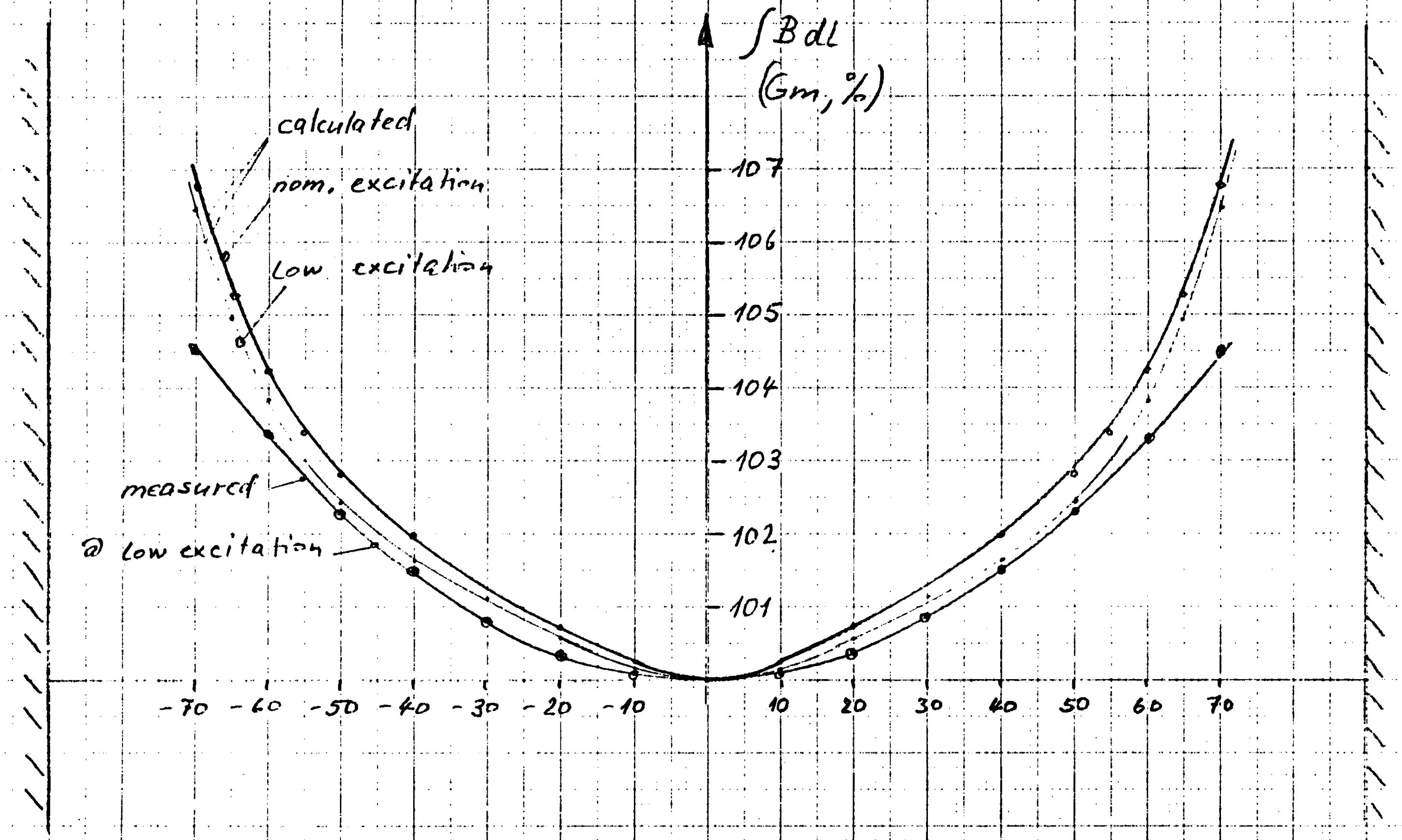

Fig. 4. ∫Bdl across aperture on centre line

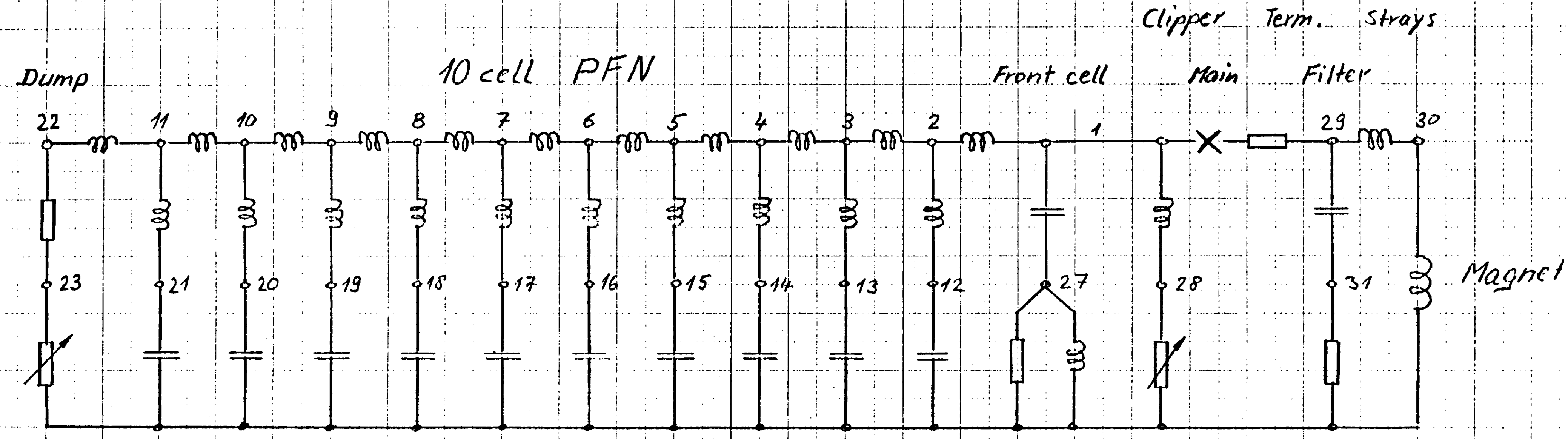

Fig. 5. Detailed circuit used for computation with ECAP

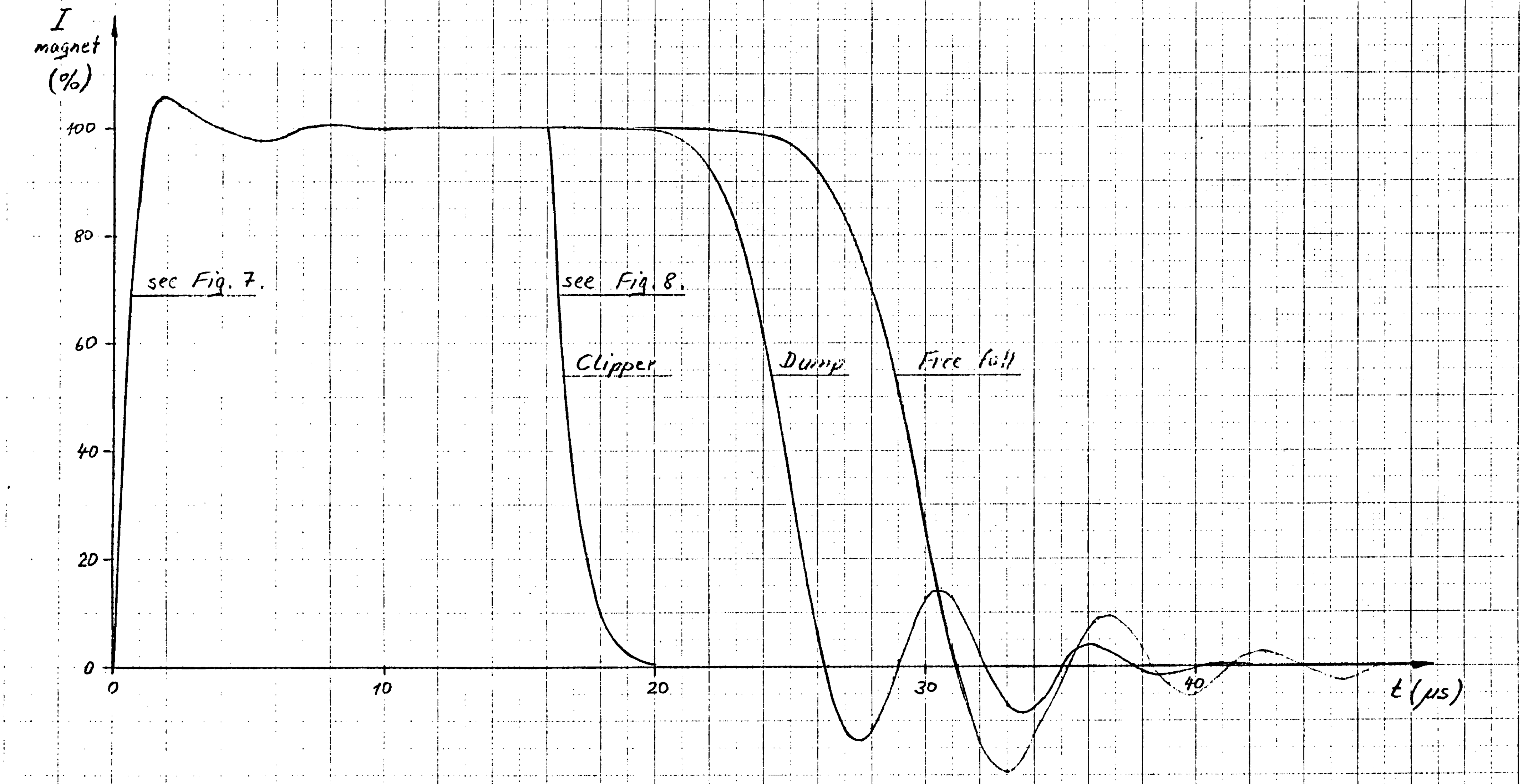

Fig. 6. Typical magnet current pulse waveforms (ECAP)

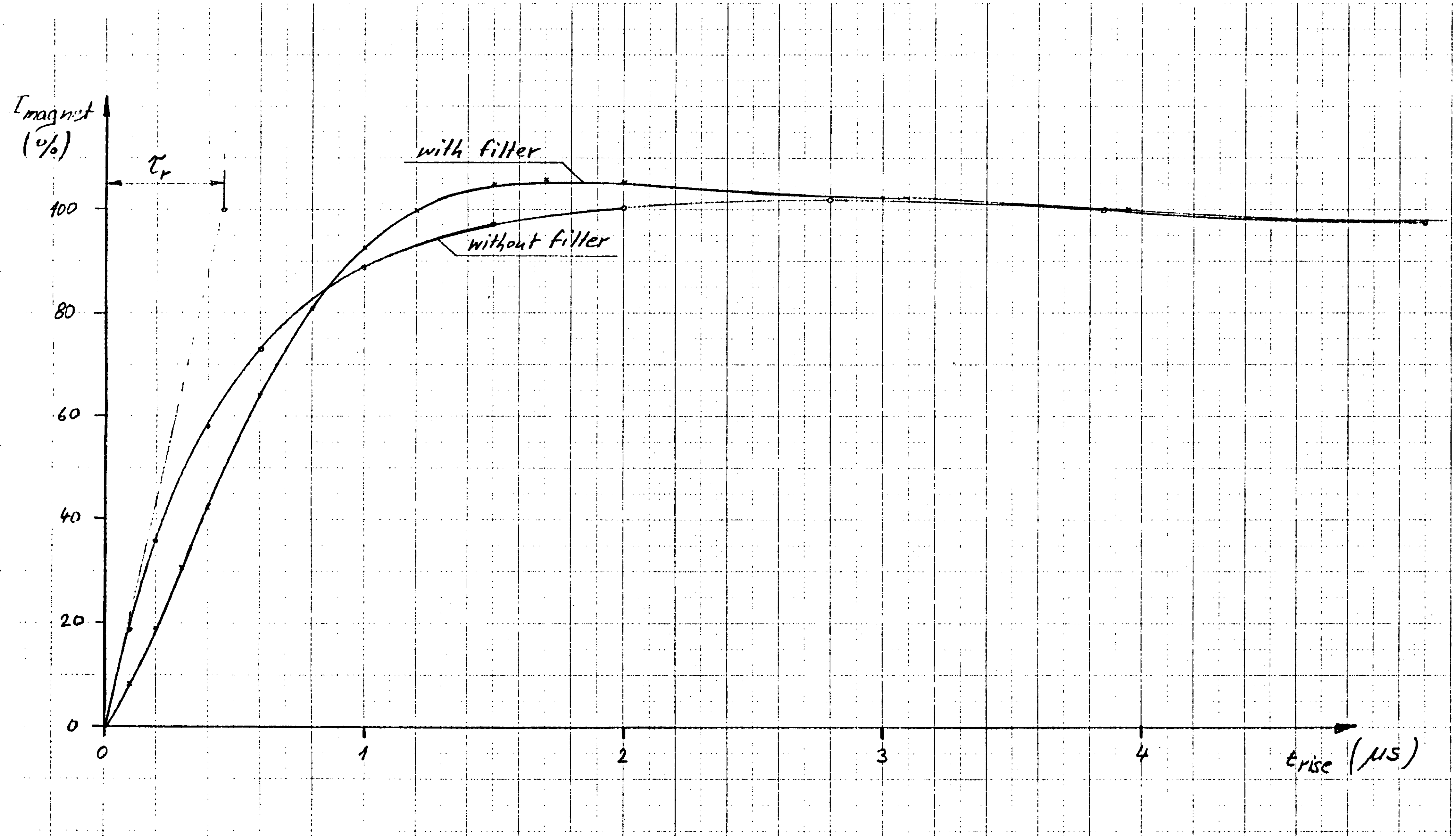

Fig. 7. Detail of magnet current rise (ECAP)

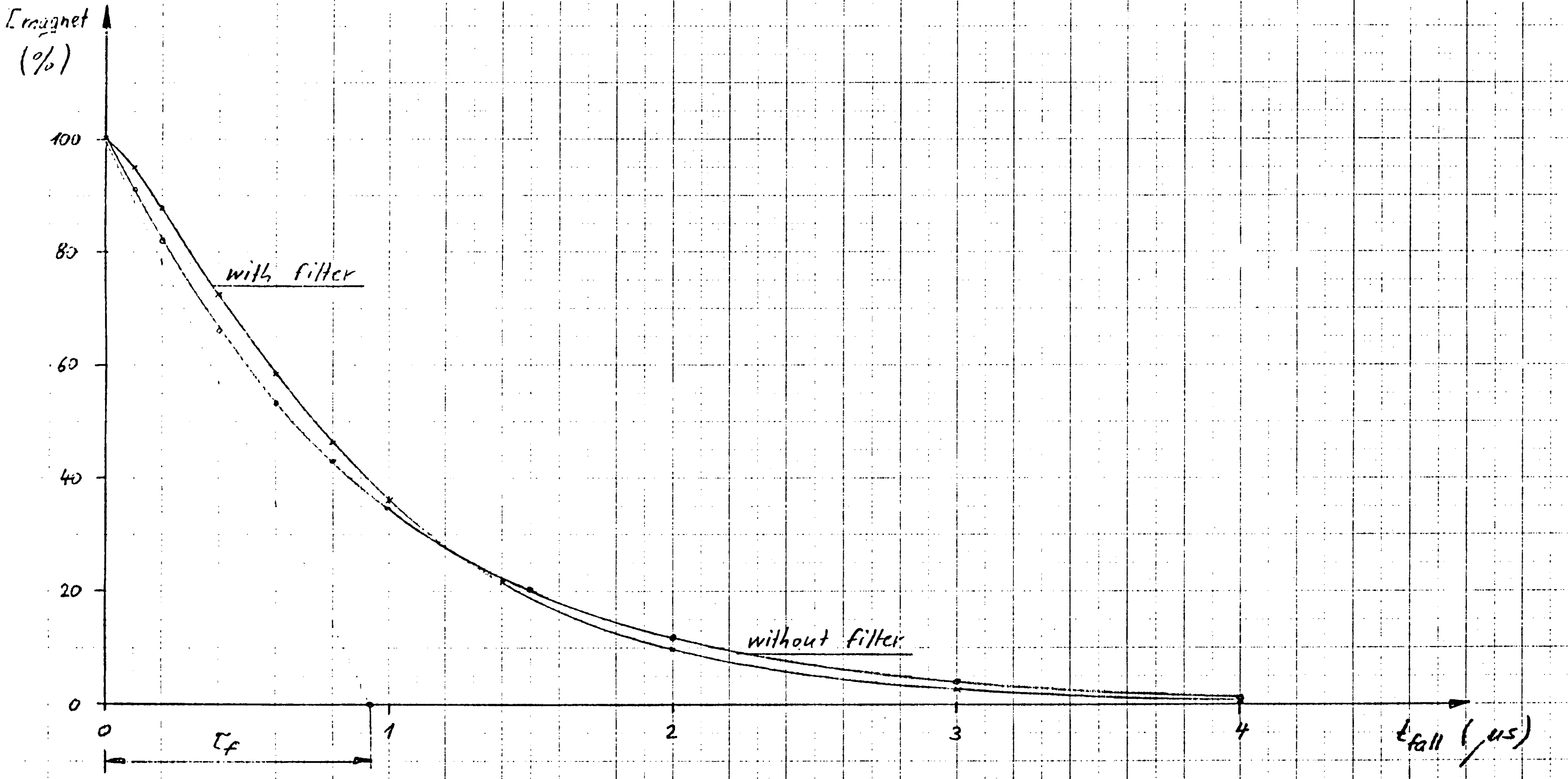

Fig. 8. Detail of magnet current fall (ECAP)